

# Temporal-spatial cross-correlation analysis of non-stationary near-surface wind speed time series

ZENG Ming(曾明), LI Jing-hai(李静海), MENG Qing-hao(孟庆浩), ZHANG Xiao-nei(张小内)

Institute of Robotics and Autonomous Systems, Tianjin Key Laboratory of Process Measurement and Control  
(School of Electrical Automation and Information Engineering, Tianjin University), Tianjin 300072, China

© Central South University Press and Springer-Verlag Berlin Heidelberg 2017

**Abstract:** Temporal-spatial cross-correlation analysis of non-stationary wind speed time series plays a crucial role in wind field reconstruction as well as in wind pattern recognition. Firstly, the near-surface wind speed time series recorded at different locations are studied using the detrended fluctuation analysis (DFA), and the corresponding scaling exponents are larger than 1. This indicates that all these wind speed time series have non-stationary characteristics. Secondly, concerning this special feature (i.e., non-stationarity) of wind signals, a cross-correlation analysis method, namely detrended cross-correlation analysis (DCCA) coefficient, is employed to evaluate the temporal-spatial cross-correlations between non-stationary time series of different anemometer pairs. Finally, experiments on ten wind speed data synchronously collected by the ten anemometers with equidistant arrangement illustrate that the method of DCCA cross-correlation coefficient can accurately analyze full-scale temporal-spatial cross-correlation between non-stationary time series and also can easily identify the seasonal component, while three traditional cross-correlation techniques (i.e., Pearson coefficient, cross-correlation function, and DCCA method) cannot give us these information directly.

**Key words:** temporal-spatial cross-correlation; near-surface wind speed time series; detrended cross-correlation analysis (DCCA); cross-correlation coefficient; Pearson coefficient; cross-correlation function

## 1 Introduction

Since near-surface wind is governed by a variety of physical processes and complex surface topography, wind signals are extremely inhomogeneous both in temporal and spatial scales. Therefore, studying the temporal-spatial characteristics of near surface wind is an interesting and challenging task.

Numerous studies have focused on the temporal correlation (i.e., long term correlation) of wind speed records over the last decade [1–8]. Compared with temporal research works, few studies addressed on temporal-spatial cross-correlation in terms of fractal theory. Accurate measurement of the temporal-spatial cross-correlation of near-surface wind will be benefit for numerous applications. For the application of wind field reconstruction [9], reconstruction accuracy strongly depends on the accurate temporal-spatial cross-correlation between wind data collected at different locations. For the application of wind pattern recognition [10], temporal-spatial cross-correlation between wind data provides important clues for measuring the level of

similarity between the testing pattern and the predefined pattern.

Pearson coefficient and cross-correlation function are two popular methods to investigate the cross-correlation between time series. However, these two techniques have certain limitations. In terms of Pearson coefficient, it is a global metric, and for non-zero correlations it is a biased estimator and the bias increases with increasing strength of non-stationarity [11]. As for cross-correlation function, recent studies [12] state that it can be employed to reveal the time dynamic causality, but it is also not suited for non-stationary signals. In the real world, many data are highly non-stationary. To address the non-stationary problem, the method of detrended cross-correlation analysis (DCCA) [13] was proposed. This method can quantify long-range power-law cross-correlations, while it cannot quantify the level of cross-correlations. In order to overcome the shortcoming of DCCA, a new method, called DCCA cross-correlation coefficient [14], was proposed. This technique not only quantifies the level of cross-correlation between non-stationary time series but also identifies seasonal components. Therefore, we prefer

**Foundation item:** Projects(61271321, 61573253, 61401303) supported by the National Natural Science Foundation of China; Project(14ZCZDSF00025) supported by Tianjin Key Technology Research and Development Program, China; Project(13JCYBJC17500) supported by Tianjin Natural Science Foundation, China; Project(20120032110068) supported by Doctoral Fund of Ministry of Education of China

**Received date:** 2015–11–03; **Accepted date:** 2016–12–01

**Corresponding author:** ZENG Ming, Associate Professor, PhD; Tel: +86–13114806460; E-mail: zengming@tju.edu.cn

to use DCCA cross-correlation coefficient to analyze the temporal-spatial cross-correlation between non-stationary near-surface wind speed time series. To demonstrate the effectiveness of DCCA cross-correlation coefficient, Pearson coefficient and cross-correlation function as well as DCCA are utilized for comparisons. In experimental sets, ten high precision 2D ultrasonic anemometers (UAs) are deployed in line with 1 m interval (see Fig. 1). Note that this arrangement of sensors can easily check the accuracy and robustness of different cross-correlation estimators.

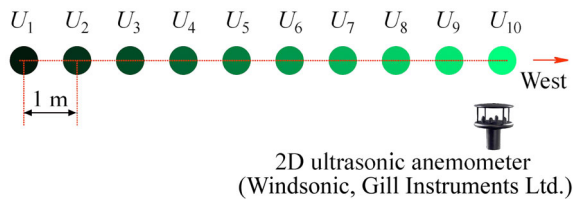


Fig. 1 Deployment of ten 2D ultrasonic anemometers

## 2 Methodology

Detrended cross-correlation coefficient [14] is a newly developed method to quantify the cross-correlation between two non-stationary time series. It is a combination of DCCA [13] and detrended fluctuation analysis (DFA) [15], and it has been successfully applied to various fields including economics, geography, meteorology, as well as engineering [8, 16–20]. A detailed description of DCCA cross-correlation coefficient algorithm can be found in Refs. [11, 14, 21]. Here, the procedure is briefly described as follows.

Considering two time series  $\{x_i\}$  and  $\{y_i\}$  with equal length  $N$ , we construct the “profile” of each series by integrating these time series, obtaining  $X_k = \sum_{i=1}^k (x_i - \bar{x})$  and  $Y_k = \sum_{i=1}^k (y_i - \bar{y})$ ,  $k=1, 2, \dots, N$ , where  $\bar{x}$  and  $\bar{y}$  denote the global average of  $\{x_i\}$  and  $\{y_i\}$ . Then, two profiles are divided into  $N-s$  overlapping boxes with equal length  $s$ , each starting at  $i$  and ending at  $i+s$ , in other words, each containing  $s+1$  values. For both time series, in the  $v$ -th box that starts at  $i$  and ends at  $i+s$ , we define the “local trend”  $\tilde{X}_{k,v}$  and  $\tilde{Y}_{k,v}$  ( $i \leq k \leq i+s$ ,  $v=1, 2, \dots, N-s$ ) to be the ordinate of a linear least-squares fit. The “detrended walk” comes to be the difference between the original walk and the local trend. The detrended covariance of the residuals in each box is defined as  $f_{DCCA}^2(s, v) = 1/(s+1) \sum_{k=i}^{i+s} (X_k - \tilde{X}_{k,v}) \cdot (Y_k - \tilde{Y}_{k,v})$ . Next, we calculate the DCCA covariance function by averaging  $f_{DCCA}^2(s, v)$  over all overlapping  $N-s$  boxes of size  $s$ ,

$$F_{DCCA}^2(s) = \frac{1}{N-s} \sum_{i=1}^{N-s} f_{DCCA}^2(s, i) \tag{1}$$

If the two series are long-range cross-correlated, then cross-correlations decay as a power law, the corresponding detrended covariance is either always positive or always negative, and DCCA covariance function grows with time scale  $s$  as

$$F_{DCCA}(s) \sim s^\lambda \tag{2}$$

The exponent  $\lambda$ , which describes the power-law relationship between two series, is obtained as the slope of the least square line fitting of  $\lg[F_{DCCA}(s)]$  versus  $\lg[s]$ . Supposing  $\{x_i\} = \{y_i\}$ , the detrended covariance  $F_{DCCA}^2(s)$  reduces to the detrended variance  $F_{DFA}^2(s)$  used in the DFA method. In this case, the exponent is equivalent to the well-known Hurst exponent  $H$ , which takes values between 0 and 1 for stationary processes, while takes  $1 < H < 1.5$  for non-stationary processes [22]. Finally, based on DFA fluctuation function and DCCA covariance function, we can calculate the cross-correlation coefficient by

$$\rho_{DCCA}(s) = \frac{F_{DCCA}^2(s)}{F_{DFA,x}(s)F_{DFA,y}(s)} \tag{3}$$

The primary advantage of the DCCA cross-correlation coefficient is that it’s capable of measuring the true correlation levels between two non-stationary time series at different time scales [14, 21]. PODOBNIK et al [21] showed that  $\rho_{DCCA}$  bounded between  $-1$  and  $1$ , and  $\rho_{DCCA}=1$  for perfectly correlated series,  $\rho_{DCCA}=0$  for uncorrelated series,  $\rho_{DCCA}=-1$  for perfectly anti-correlated processes.

## 3 Experimental settings

The wind data are collected at an open space in Tianjin University, located at N39.06°, E117.09°. Ten high-precision 2D UAs (WindSonic, Gill Instruments Ltd.) are deployed in line with interval of 1 m and are elevated 0.6 m above the ground. Sampling rate is 4 Hz and recording duration is 1 h. Therefore, the data for each sensor are 14400 points. For simplicity, we use  $U_1-U_{10}$  to represent 10 UAs, respectively.

## 4 Experimental results and discussion

### 4.1 Verification of wind data having fractal and non-stationary characteristics

The measurement results of ten 2D UAs are shown in Fig. 2, indicating that all wind speed time series look similar, whereas each one fluctuates in an irregular and complex manner. Firstly, DFA method is adopted to verify whether wind speed data show temporal fractal behavior at high-resolution temporal (second) scales. The log-log plots of the DFA fluctuation functions versus time scale  $s$  are illustrated in Fig. 3(a), demonstrating

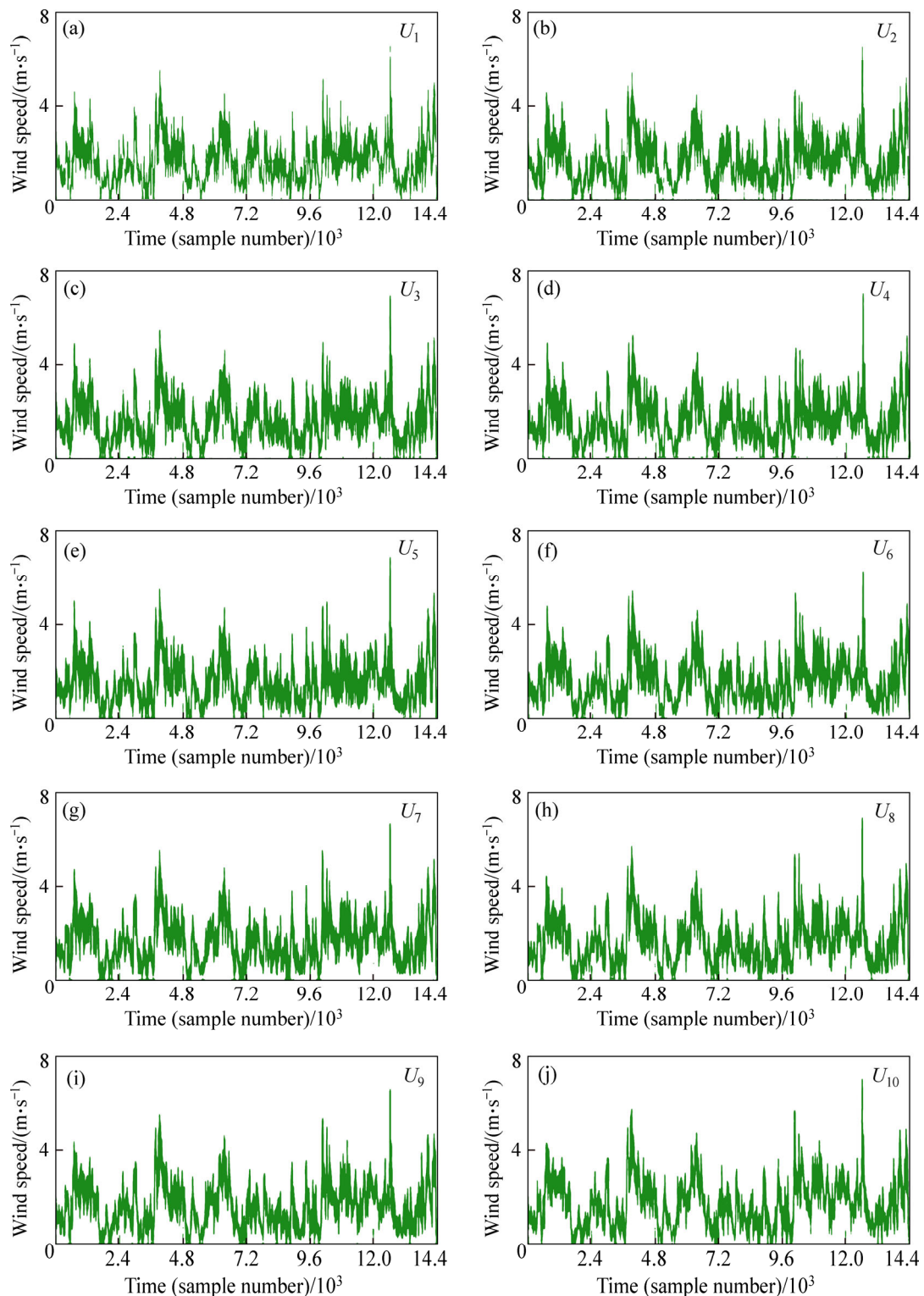


**Fig. 2** Measurements of ten 2D ultrasonic anemometers (The wind time series are simultaneously recorded with 4 Hz sampling rate during a period of 1 h and each series contains 14400 points)

that all fluctuation functions scale as a power law for a broad range of time scales ( $8 < s < 2880$ , i.e., range from 2 s to 360 s). All corresponding scaling exponents are greater than 1 ( $H \approx 1.2$ , see Fig. 3(b)), which indicates that the dynamic of the wind speed shows persistence properties at second scales and all wind speed time series

have non-stationary features [22].

In order to further test the scaling behavior of non-stationary time series, surrogate time series are generated by shuffling the original wind speed records [2, 3, 23]. The test results show that those new surrogate data preserve the distribution of the original ones, while the

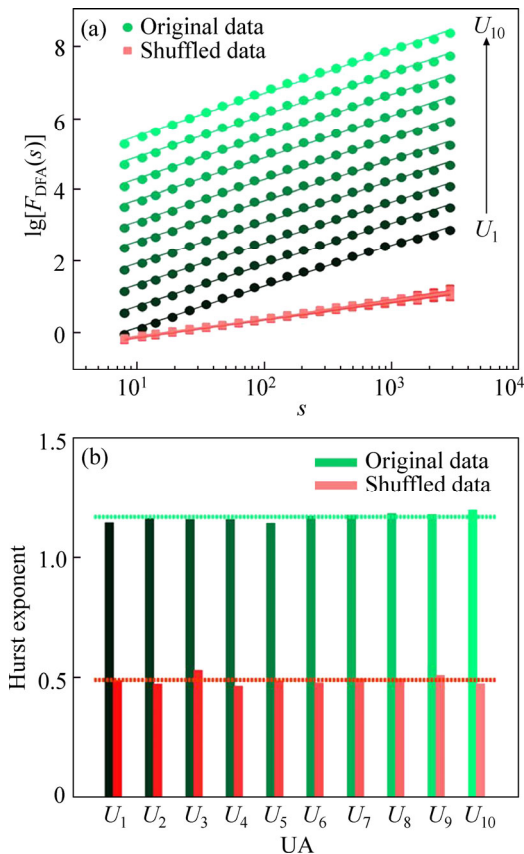


**Fig. 3** Results of DFA analysis: (a) All fluctuation functions of original data and shuffled data showing similar power law behaviors; (b) Statistic results of Hurst exponents for original data ( $H \approx 1.2$ ) and shuffled data ( $H = 0.5$ ) (Different gradient colors represent different UAs. The DFA fluctuation functions for original data are vertically shifted for clarity)

corresponding long range correlations are destroyed, as shown in Fig. 3(a). Statistical results in Fig. 3(b) illustrate that the shuffling signals exhibit uncorrelated behavior ( $H = 0.5$ , i.e., white noise). Abovementioned analysis confirms that the scaling behavior of near-surface wind speed is due to the temporal correlations, rather than the distribution.

### 4.2 Temporal-spatial cross-correlation analysis using conventional techniques

The wind speed time series are measured simultaneously from the ten 2D UAs deployed in line with 1 m interval as shown in Fig. 2. We set  $U_1$  as the reference location. Next, three conventional methods, i.e., Pearson coefficient, cross-correlation function and DCCA are implemented to evaluate the spatial cross-correlation between the  $U_1$  and other  $U_x (U_1 \times U_x, x = 2, 3, \dots, 10)$ .

#### 4.2.1 Analysis results by Pearson coefficient

The spatial cross-correlation levels between the  $U_1$  and other nine  $U_x$  (i.e.,  $U_1 \times U_x, x = 2, 3, \dots, 10$ ) using the method of Pearson coefficient are 0.9191, 0.8797, 0.8467,

0.8077, 0.7956, 0.7771, 0.7568, 0.7319, 0.7117, respectively (see Fig. 4). In this figure we can identify that there indeed exist strong spatial cross-correlations between the referenced  $U_1$  and other  $U_x$ , and the corresponding intensity value increases with a decrease in the intervals. Due to the intrinsic limitation of the Pearson coefficient, this method only provides the global measurement of the level of the spatial cross-correlation. In other words, this analysis cannot reflect the cross-correlation variance as a function of the time scales.

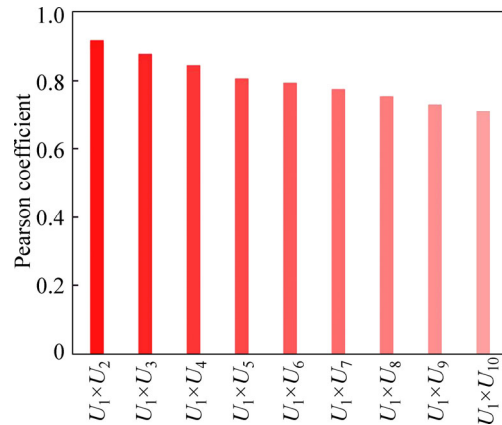


**Fig. 4** Test results using Pearson coefficient

#### 4.2.2 Test results by cross-correlation function

Next, cross-correlation function is adopted to evaluate the spatial variability of wind speed data. The highlight of this method is that it is capable of measuring the distinction between two time series as a function of the lag time. This technique can be implemented as the convolution of two series  $\{x_i\}$  and  $\{y_i\}$ , and the cross-correlation function is calculated as  $C(\tau) = \sum_{i=-\infty}^{\infty} x_i^* y_{i+\tau}$  ( $i = 1, 2, \dots, N$ ), where  $x_i^*$  denotes the complex conjugate of  $x_i$ , and  $\tau$  is the lag parameter.

Compared with the standard Pearson coefficient, the superiority of the cross-correlation function is that it concerns about the time lag problem. When  $\tau = 0$  (no delay), the cross-correlation results agree well with the deployment of UAs. Besides, the cross-correlation levels  $C(\tau)$  decay with the time lag  $\tau$ . However, except for  $\tau = 0$ , there is no stable relationship between the intensities of  $C(\tau)$  and the deployment of UAs, and in most cases, the values of  $C(\tau)$  for different  $U_x (x = 2, 3, \dots, 10)$  vary slightly at the same  $\tau$ , as shown in Fig. 5.

#### 4.2.3 Analysis results by DCCA method

Concerning about the non-stationary features of the signals, a new strategy, called detrended cross-correlation analysis method (DCCA) was developed to study cross-correlation between time series. Taking into account the fractal and non-stationary characteristics in wind speed data (see Section 4.1), we therefore apply DCCA method to investigate cross-correlations between

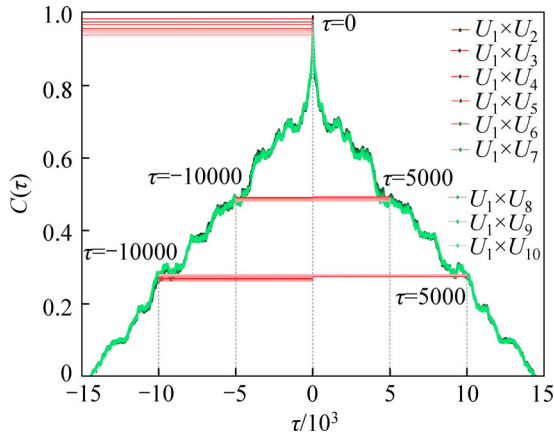


**Fig. 5** Test results using cross-correlation function (Except for  $\tau=0$ , there is no stable relationship between the intensities of  $C(\tau)$  and deployment of UAs, and in most cases ( $\tau \neq 0$ ), there is little difference in  $C(\tau)$  for different UAs, such as  $\tau=-10000, -5000, 5000, 10000$ )

the  $U_1$  and other  $U_x$ .

Figure 6 exhibits DCCA results in log-log scale. Cross-correlations between the  $U_1$  and other UAs are all very well fitted by power laws (Fig. 6(a)) with  $\lambda_i=1.1853, 1.1942, 1.2014, 1.1971, 1.2134, 1.2179, 1.2204, 1.2208,$

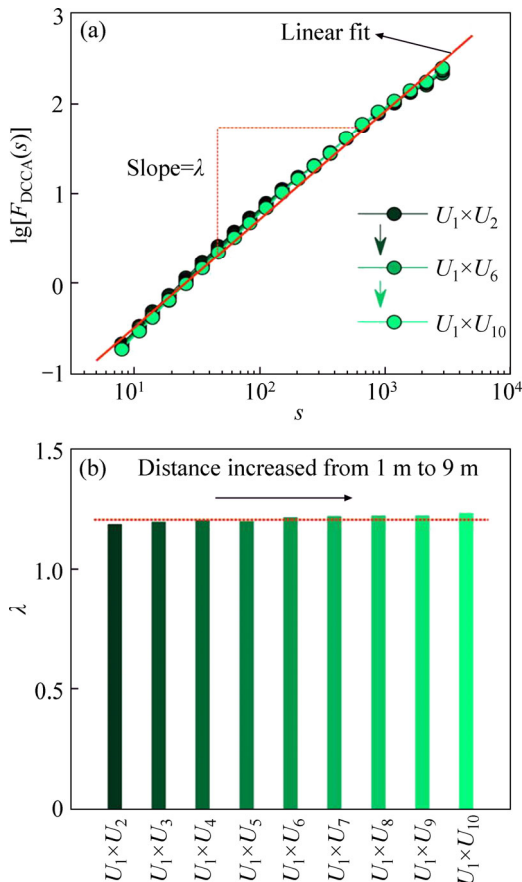


**Fig. 6** Cross-correlation results between  $U_1$  and other  $U_x$  using DCCA technique: (a) Fluctuation functions of DCCA very well fitted by power-laws; (b) Cross-correlation  $\lambda$  exponents similar for different sensor pairs

1.2306 for  $U_1 \times U_x$  ( $x=2, 3, \dots, 10$ ), respectively (see Fig. 6(b)). This figure informs us that if we analyze the cross-correlation between the  $U_1$  and other  $U_x$  utilizing the DCCA method, we have the similar behaviors with little difference. It is obvious that the DCCA method can quantify long-range power-law cross-correlations, while it cannot quantify the level of cross-correlations in function of time scale  $s$ .

**4.3 Test results by DCCA cross- correlation coefficient**

In order to overcome the limitation of DCCA, ZEBENDE [14] proposed a novel modified method, i.e., DCCA cross-correlation coefficient which is defined as the ratio between the detrended covariance function and the detrended variance function. The main advantages of this proposed method, compared with the DCCA strategy, is that it can quantify the level of cross-correlation as a function of time scales as well as can easily identify the seasonal components.

Next, the DCCA cross-correlation coefficients are calculated between the  $U_1$  and other  $U_x$  (see  $\rho_{DCCA}$  in Fig. 7). The corresponding cross-correlations are always

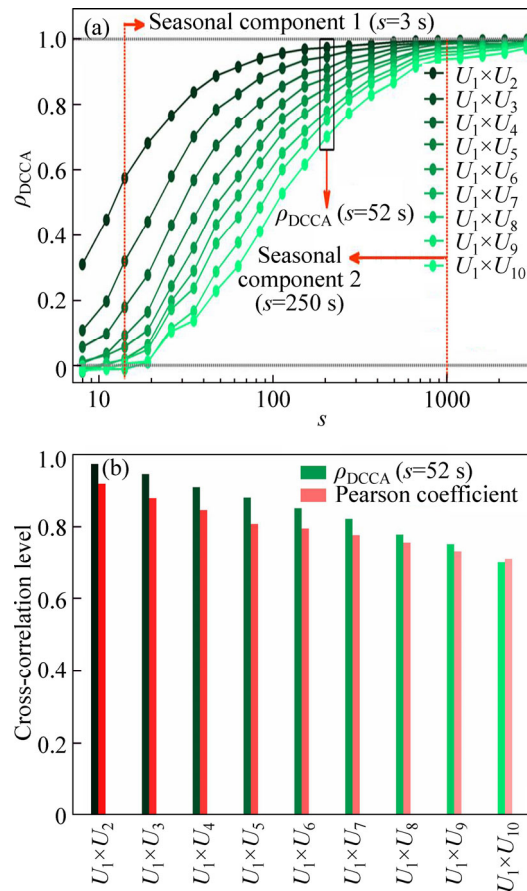


**Fig. 7** Results using DCCA cross-correlation coefficient: (a) Cross-correlations between  $U_1$  and other  $U_x$  exhibit different behaviors in terms of time scale  $s$  and corresponding offsets of cross-correlation are in agreement with spatial relationship between  $U_1$  and other  $U_x$ ; (b) Analysis results of Pearson coefficient similar to results of  $\rho_{DCCA}$  at  $s=204$  (52 s)

positive and not perfect until  $s \approx 1000$  (250 s). In most cases, starting from lower levels of cross correlation ( $\rho_{DCCA} \leq 0.3$ ) at the small time scales ( $s \leq 12$ , i.e., 3 s), they will transfer to perfect cross-correlation ( $\rho_{DCCA} \approx 1$ ) at large time scales ( $s \geq 1000$ , i.e., 250 s). That is why we cannot use only the DCCA method to quantify the level of cross-correlation.

In contrast to the results of DCCA, the cross-correlations between the  $U_1$  and other  $U_x$  exhibit different behaviors in terms of time scale  $s$  and in most cases the offsets of cross-correlation for different sensor pairs are in agreement with the spatial arrangement of  $U_x$  shown in Fig. 1. In other words, the smaller the distance to  $U_1$  is, the larger the cross-correlation there will be at a certain time scale (see Fig. 7(a)). This figure also informs us an important fact that the spatial cross-correlations between the  $U_1$  and other UAs change according to the time scale  $s$ . These results may have far-reaching consequences for wind field reconstruction and wind forecasting. Moreover, in Fig. 7(a) we can identify the seasonal components, i.e.,  $s=12$  (3 s) divides  $\rho_{DCCA}$  into weak cross-correlation ( $s < 12$ ) or not ( $s > 12$ ), and  $s=1000$  (250 s) divides  $\rho_{DCCA}$  into perfect cross-correlation ( $s > 1000$ ) or not ( $s < 1000$ ). Finally, compared with the measurement of Pearson coefficient (see Fig. 7(b)), similar results are found at certain time scale ( $s=204$ , i.e., 52 s) in Fig. 7(a).

## 5 Conclusions

1) The temporal-spatial cross-correlation between the time series recorded at different locations has many potential applications. However, tests on ten wind-speed data of anemometers with regular arrangement show that the conventional methods of cross-correlation, such as Pearson coefficient, cross-correlation function and DCCA, are unsuitable to measure the temporal-spatial cross-correlation between the wind speed time series. Pearson coefficient and DCCA are single metric techniques, thus for the cases in which the temporal-spatial cross-correlation changes as the time scale changes, these two methods failed. The cross-correlation results using cross-correlation function are fluctuated in many cases, which are not well matched with the regular arrangement of UAs.

2) Taking into account the non-stationary features of wind speed time series, a state-of-art method, called DCCA cross-correlation coefficient, was applied to analyze the cross-correlation between the different sensor pairs. The experimental results show that this method can accurately quantify the level of cross-correlation between non-stationary wind speed time series and also successfully identify the seasonal component. Next, we plan to use this robust method to do the works of the wind field reconstruction based on real measurement and wind pattern recognition.

## References

- [1] GOVINDAN R B, KANTZ H. Long-term correlations and multifractality in surface wind speed [J]. *Europhysics Letters*, 2004, 68(2): 184–190.
- [2] KAVASSERI R G, NAGARAJAN R. Evidence of crossover phenomena in wind-speed data [J]. *IEEE Transactions on Circuits and Systems*, 2004, 51(11): 2255–2262.
- [3] KAVASSERI R G, NAGARAJAN R. A multifractal description of wind speed records [J]. *Chaos Solitons & Fractals*, 2005, 24(1): 165–173.
- [4] KOCAK K. Examination of persistence properties of wind speed records using detrended fluctuation analysis [J]. *Energy*, 2009, 34(11): 1980–1985.
- [5] FENG Tao, FU Zun-tao, DENG Xing, MAO Jiang-yu. A brief description to different multi-fractal behaviors of daily wind speed records over China [J]. *Physics Letters A*, 2009, 373(45): 4134–4141.
- [6] TELESCA L, LOVALLO M. Analysis of the time dynamics in wind records by means of multifractal detrended fluctuation analysis and the Fisher-Shannon information plane [J]. *Journal of Statistical Mechanics-Theory and Experiment*, 2011, 2011(7): 07001.
- [7] SANTOS M D O, STOSIC T, STOSIC B D. Long-term correlations in hourly wind speed records in Pernambuco, Brazil [J]. *Physica A*, 2012, 391: 1546–1552.
- [8] ANJOS P S D, SILVA A S A D, STOSIC B, STOSIC T. Long-term correlations and cross-correlations in wind speed and solar radiation temporal series from Fernando de Noronha Island, Brazil [J]. *Physica A*, 2015, 424: 90–96.
- [9] BECK V, DOTZEK N. Reconstruction of near-surface tornado wind fields from forest damage [J]. *Journal of Applied Meteorology and Climatology*, 2010, 49(7): 1517–1537.
- [10] AZAD H B, MEKHILEF S, GANAPATHY V G. Long-term wind speed forecasting and general pattern recognition using neural networks [J]. *IEEE Transactions on Sustainable Energy*, 2014, 5(2): 546–553.
- [11] KRISTOUFEK L. Measuring correlations between non-stationary series with DCCA coefficient [J]. *Physica A*, 2014, 402: 291–298.
- [12] CHEN Yan-guang. A new methodology of spatial cross-correlation analysis [J]. *PLOS ONE*, 2015, 10(5): 01261585.
- [13] PODOBNIK B, STANLEY H E. Detrended cross-correlation analysis: A new method for analyzing two nonstationary time series [J]. *Physical Review Letters*, 2008, 100(8): 38–71.
- [14] ZEBENDE G F. DCCA cross-correlation coefficient: Quantifying level of cross-correlation [J]. *Physica A*, 2011, 390(4): 614–618.
- [15] PENG C K, BULDYREV S V, HAVLIN S, SIMONS M, STANLEY H E, GOLDBERGER A L. Mosaic organization of DNA nucleotides [J]. *Physical Review E*, 1994, 49(2): 1685–1689.
- [16] da SILVA M F, de AREA LEAO PEREIRA E J, da SILVA FILHO A M, MIRANDA J G V, ZEBENDE G F. Quantifying cross-correlation between Ibovespa and Brazilian blue-chips: The DCCA approach [J]. *Physica A*, 2015, 424: 124–129.
- [17] DONG Ke-qiang, FAN Jie, GAO You. Cross-correlations and structures of aero-engine gas path system based on DCCA coefficient and rooted tree [J]. *Fluctuation and Noise Letters*, 2015, 2(14): 1550014.
- [18] DONG Ke-qiang, GAO You, JING Li-ming. Correlation tests of the engine performance parameter by using the detrended cross-correlation coefficient [J]. *Journal of the Korean Physical Society*, 2015, 66(4): 539–543.
- [19] CAO Guang-xi, HAN Yan. Does the weather affect the Chinese stock

- markets? Evidence from the analysis of DCCA cross-correlation coefficient [J]. *International Journal of Modern Physics B*, 2015, 29(01): 14502361.
- [20] SHEN Chen-hua, LI Chao-ling, SI Ya-li. A detrended cross-correlation analysis of meteorological and API data in Nanjing, China [J]. *Physica A*, 2015, 419: 417–428.
- [21] PODOBNIK B, JIANG Zhi-qiang, ZHOU Wei-xing, STALEY H E. Statistical tests for power-law cross-correlated processes [J]. *Physical Review E*, 2011, 84: 066118.
- [22] KRISTOUFEK L. Power-law correlations in finance-related Google searches, and their cross-correlations with volatility and traded volume: Evidence from the Dow Jones Industrial components [J]. *Physica A*, 2015, 428: 194–205.
- [23] IVANOV P C, AMARAL L, GOLDBERGER A L, HAVLIN S, ROSENBLUM M G, STRUZIKLL Z R, STANLEY H E. Multifractality in human heartbeat dynamics [J]. *Nature*, 1999, 399(6735): 461–465.

(Edited by YANG Hua)

**Cite this article as:** ZENG Ming, LI Jing-hai, MENG Qing-hao, ZHANG Xiao-nei. Temporal-spatial cross-correlation analysis of non-stationary near-surface wind speed time series [J]. *Journal of Central South University*, 2017, 24(3): 692–698. DOI: 10.1007/s11771-017-3470-4.